Transition from classical to quantum response in semiconductor superlattices at THz frequencies

S. Zeuner, B. J. Keay, and S. J. Allen
Center for Free-electron Laser Studies, University of California at Santa Barbara, Santa Barbara, California 93106

K. D. Maranowski and A. C. Gossard
Materials Department, University of California at Santa Barbara, Santa Barbara, California 93106

U. Bhattacharya and M. J. W. Rodwell
Department of Electrical and Computer Engineering, University of California at Santa Barbara, Santa Barbara, California 93106

(Received 27 September 1995)

The response of a sequential resonant tunneling superlattice to intense THz radiation shows a transition from classical rectification at frequencies below 600 GHz to quantum response above 1 THz. In the quantum regime, the dc current-voltage characteristics show distinct peaks due to absorption and stimulated emission of up to three THz photons. For sufficiently high ac field strengths the photon-assisted channels dominate the transport, leading to absolute negative conductance near zero bias, and gain just below the Stark splitting of the ground states in adjacent quantum wells. Quantitative agreement with these observations is obtained by invoking photon-assisted tunneling following Tucker, but with an instantaneous *I-V* free of domain formation.

According to the theory of photon-assisted tunneling (PAT), single barrier tunneling devices undergo a transition from classical energy detectors to photon counters at frequencies where their conductance varies appreciably over a voltage scale given by $\hbar\omega/e$.[1] In the quantum limit the absorption of a single photon can lead to the tunneling of an additional electron, although for high field strengths multiphoton processes may become important. Photon-assisted tunneling has been studied first in superconductor-insulator-superconductor (SIS) junctions.[2] Later, features associated with PAT have been observed in nonsuperconducting systems as normal-metal point contacts,[3] and more recently, in semiconductor superlattices,[4] resonant tunneling diodes,[5] and quantum dots.[6]

In this paper we report measurements on a sequential resonant tunneling superlattice subject to intense THz fields. At frequencies above 1 THz the current-voltage characteristic shows additional peaks due to the photon-assisted transport channels, stimulated photon emission and absorption, a remarkable consequence of which is the appearance of absolute negative conductance.[7] At frequencies less than 1 THz the response is shown to roll over to classical rectification, even in a regime where the ac field is not small compared to the dc field provided by the bias voltage.

For a single tunneling barrier the standard theory of PAT assumes that the high-frequency field adiabatically changes the energy of the electrons on one side of the barrier, while the other side is held fixed as a reference. The tunneling current in the presence of the ac field, $I_{\rm irr}(V)$, can then be expressed in terms of the dc *I-V* without radiation, $I_0(V)$, by[1,8]

$$I_{\rm irr}(V)=\sum_{n=-\infty}^{\infty} J_n^2(\alpha) I_0(V+n\hbar\omega/e) \tag{1}$$

with $\alpha=eE_{\rm ac}b/\hbar\omega$. Here, $E_{\rm ac}$ is the ac field strength, b is the barrier thickness, and J_n is the ordinary Bessel function of order n. The irradiated *I-V* has the form of a sum of the dc *I-V* curves I_0, displaced by a voltage corresponding to an integer number of photon energies, and weighted by $J_n^2(\alpha)$, a nonmonotonic function of the ac field. Prominent features of the dc *I-V* are expected to appear in the irradiated *I-V* displaced by $\pm\hbar\omega/e$, $\pm 2\hbar\omega/e$ and so on, where the relative size of these replicas depends on the ac field strength. It can be seen from Eq. (1) that nonlinear effects become important if $\alpha \gtrsim 1$, i.e., if the voltage drop across the barrier due to the ac field becomes comparable to the photon energy. For frequencies around 1 THz and typical barrier dimensions this requires a field strength of several kV/cm.

For low frequencies, where $\hbar\omega/e$ is smaller than the voltage scale of the dc nonlinearity, the photon replicas of the dc *I-V* curve are too close together to be distinguishable. In the low-frequency limit Eq. (1) reduces to the classical rf detection formula,[9]

$$I_{\rm rf}(V)=\frac{1}{\pi}\int_0^{\pi} I_0(V+V_{\rm ac}\cos\omega t)\,d(\omega t), \tag{2}$$

where $V_{\rm ac}=E_{\rm ac}b$ is the voltage drop across the barrier.

Equation (1) was originally derived for SIS junctions[8] but is believed to be valid for any two-terminal tunneling device where the electron wave functions on both sides of the barrier are incoherent; each electron passes the system in a single leap, and the leaps of different electrons are uncorrelated.[10]

The 10 period GaAs/$Al_xGa_{1-x}As$ ($x=0.3$) superlattice used in these experiments was grown on a semi-insulating GaAs substrate by molecular-beam epitaxy. It consists of 10 150-Å GaAs quantum wells and 11 50-Å $Al_xGa_{1-x}As$ barriers, lightly doped to $n\sim 3\times 10^{15}$ cm^{-3}, sandwiched between 500-Å spacer layers (GaAs, $n\sim 3\times 10^{15}$ cm^{-3}) and 3000-Å heavily doped contact regions (GaAs, $n^+\sim 2\times 10^{18}$ cm^{-3}). Reactive ion etching and ion implantation were used to define 2×4-μm^2 mesas. NiAuGe Ohmic contacts connected the

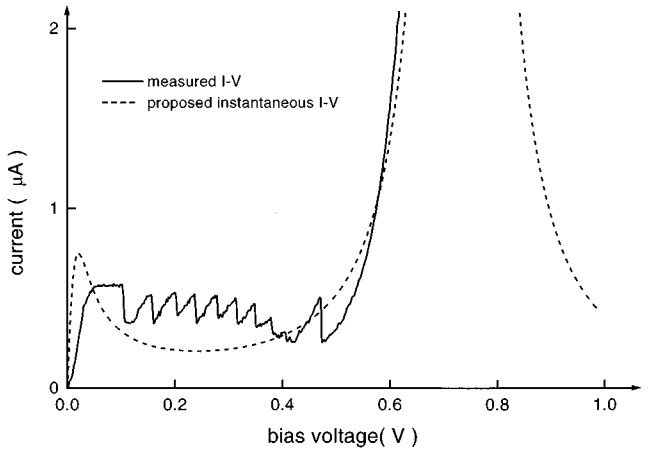

FIG. 1. Experimental dc current-voltage characteristics, measured on a time scale of 1 μs (solid line) and proposed instantaneous I-V, valid for a ps time scale.

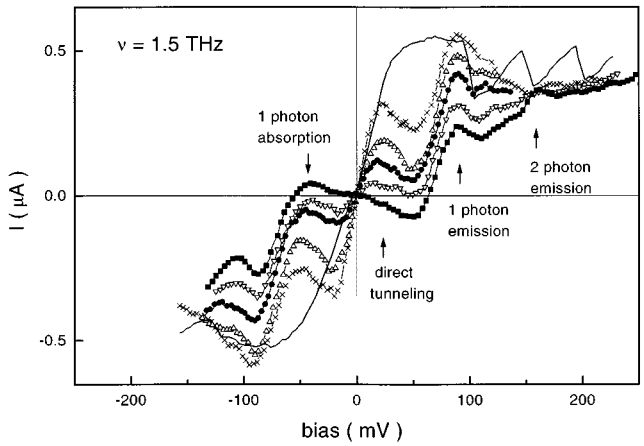

FIG. 2. Unirradiated I-V (solid line) and current-voltage characteristics measured in intense 1.5 THz fields. The laser power increases from the top to the bottom trace by a factor of 4. Prominent features are labeled according to the photon-assisted transport channels involved. As the superlattice structure is symmetric, each peak has an associated symmetry related peak at the opposite bias voltage.

top and bottom contact regions to the bows of a broadband bow tie antenna, and gold wires were bonded to the two gold bows to provide the dc bias voltage. The sample was glued on a hemispherical Si lens and mounted in a temperature variable optical cryostat. The experiments were performed between 2 K and 250 K, while most of the reported data was taken at 5 K. Our radiation source are the UCSB free-electron lasers, which provide several kilowatts of tunable radiation from 120 GHz to 4.8 THz in μs-long pulses.

Figure 1 shows the measured dc I-V of the sample. The intrinsic ground-state bandwidth of the superlattice is only $\Delta E_1 = 0.5$ meV, the quantum well states are therefore localized by level width fluctuations ($\Gamma \sim 2$ meV, shown later). At low bias voltages ($V_{dc} < 0.1$ V) the transport is governed by sequential resonant tunneling from ground state to ground state.[11] For an ideal two-dimensional system tunneling is highly restricted by the conservation of momentum in the plane of the quantum well. However, level broadening due to well-width fluctuations allows tunneling even with complete in-plane momentum conservation for bias voltages small enough that the broadened levels in adjacent wells overlap in energy.

At higher bias the dc I-V shows the typical sawtooth oscillations associated with the formation and expansion of a high-field domain.[11] In this domain the electrons tunnel from the ground state of one well to the first excited state of the neighboring well. Each time an additional well breaks off into the high-field domain, the current through the structure has to redistribute, resulting in $(N-1)$ negative conductance spikes in the dc I-V, where $N = 10$ is the number of quantum wells. Eventually, all wells are contained in the high-field domain, and a significantly larger current can flow due to resonant ground-state to first excited state tunneling.

Irradiating the superlattice with intense THz radiation changes the current-voltage characteristics dramatically (see Fig. 2). The conductivity near zero bias is driven to zero and, for sufficiently high laser power, to absolute negative values.[7] At the same time, several peaks are observed that are absent in the unirradiated I-V. The position of these peaks is independent of laser power but changes with laser frequency *except* for the peak closest to the origin (located at $V_{dc} = \pm 20$ mV and labeled "direct tunneling" in Fig. 2). This peak is encountered at essentially the same bias voltage for all frequencies used. As the superlattice structure is essentially symmetric, the I-V's are point symmetric about the origin and for each peak in Fig. 2 there is a symmetry-related peak at the opposite bias voltage.

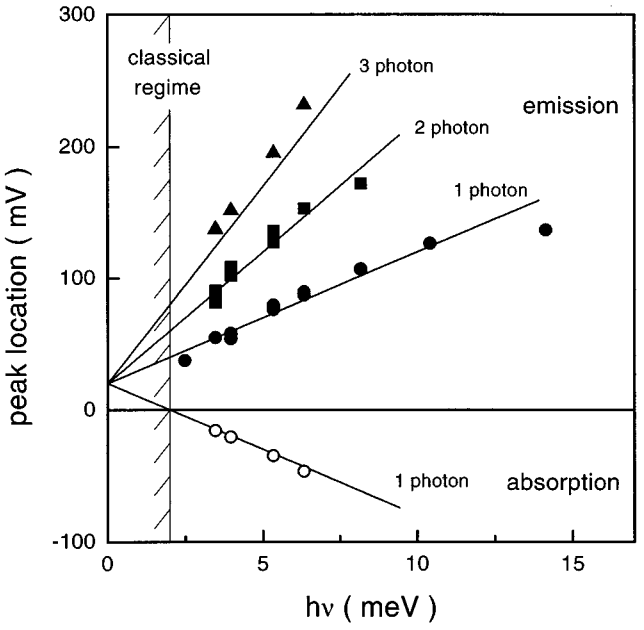

FIG. 3. Position of the prominent peaks in the irradiated I-V's as a function of the photon energy. The lines originate from $V = 20$ mV at the y axis (the position of the direct tunneling peak in Fig. 2) and have slopes of -10, $+10$, $+20$, and $+30$, corresponding to the absorption of one, and the emission of one, two, or three photons. A similar fan emerges from $V = -20$ mV, as expected by the symmetry of the I-V's. Below $h\nu = 2$ meV no features associated with photon-assisted tunneling could be observed.

In Fig. 3 the position of the peaks is plotted as a function of photon energy of the high-frequency radiation from 600 GHz (2.4 meV) to 3.5 THz (14 meV). Below 600 GHz no discernible structure could be found. The lines shown in Fig. 3 have slope -10, $+10$, $+20$, and $+30$, and intersect the y axis at 20 mV. As the superlattice consists of $N=10$ wells these lines correspond to

$$V=N(2\ \mathrm{mV}+n\hbar\ \omega/e),\quad \text{where } n=-1,\ +1,\ +2,\ \text{or } +3,$$

or to the absorption of one and the emission of up to three photons. Such a voltage dependence is to be expected for the replicas of a peak located at $N(2\ \mathrm{mV})=20$ mV in the dc I-V curve. However, the experimental dc I-V does not show any peak at the appropriate bias voltage (see Fig. 2).

To explain this discrepancy we suggest the following: The experimental dc I-V, measured on a time scale $\gtrsim 1\ \mu$s, is not the I-V curve that describes photon-assisted tunneling at high frequencies. Rather, a more intrinsic ''instantaneous'' current-voltage characteristic has to be used (see Fig. 1). We assume that this instantaneous I-V determines the response at THz frequencies through Eq. (1) and that its shape is revealed, at least for sufficiently strong ac fields, by the measurements at different laser powers and frequencies. We assume the resonant ground-state tunneling peak to occur at $V_{\mathrm{dc}}=20$ mV as suggested by the position of the frequency-independent peak in our data. This value corresponds to a level broadening due to well-width fluctuations of $\Gamma\approx 20$ meV/$N=2$ meV, consistent with a 1 ML fluctuation of the quantum well thickness. With increasing bias the voltage drop per period exceeds the level width and the conservation of in-plane momentum leads to a significant reduction of the current, until at still higher voltages the ground state and first excited state in neighboring wells are brought towards alignment.

The formation of a high-field domain takes place on a time scale of 0.1 to 1 ns (Ref. 12) and should therefore not be included in a situation where the bias voltage varies significantly with several hundred GHz. Below the threshold where the first well breaks off into the high-field domain, we expect charge buildup in the wells.[13] The lifetime in the wells can be estimated from the tunneling probability T and the number of times the electrons hit the barrier per second, $1/\tau=(v/2w)T$, where $v=(2E_1/m^*)^{1/2}$, E_1 is the ground state energy in the quantum well, and w is the well thickness.[14] Using $E_1=15$ meV and $m^*=0.067m_0$ gives τ a value of ~ 3 ns. This charge buildup is also too slow to take place during one cycle of the ac field. Eliminating these slow processes from the measured dc I-V results in the assumption of the simpler instantaneous I-V as shown in Fig. 1.

We would like to emphasize that the proposed instantaneous I-V provides a natural explanation for all the data in Figs. 2 and 3, including absolute negative conductance and gain. The peaks at $V=N(2\ \mathrm{mV}+n\hbar\omega/e)$ are now seen to be the replicas of the direct tunneling peak of the instantaneous I-V at $V=20$ mV. For photon energies larger than the level broadening, that is, for $\hbar\omega>2$ meV, the $(n=-1)$ replica of this positive peak appears at a *negative* bias voltage while the $(n=+1)$ replica of the negative direct tunneling peak at -20 mV ends up at a *positive* bias voltage. At a level of the THz radiation where the direct tunneling channel is completely suppressed [i.e., at the first zero of $J_0^2(\alpha)$], these $n=\pm 1$ replicas dominate the electron transport, as dramatically demonstrated by the occurrence of absolute negative conductance (see bottom trace in Fig. 2). For a bias above approximately $N(\hbar\omega/e)$ the current flows along the dc field but as the direct tunneling channel is suppressed, each electron in the current has to emit a photon to be able to proceed to the neighboring well. In other words, for photon energies larger than the level broadening there is absorption (negative conductance) if the Stark splitting $eE_{\mathrm{dc}}d$ between the ground states of adjacent wells is smaller than the photon energy and gain (stimulated emission) for a Stark splitting larger than $\hbar\omega$.

From Fig. 3 there seems to be an asymmetry between the strength of the absorption and emission channels (we show three emission peaks but can show only one absorption peak). This apparent asymmetry is, however, a consequence of the fact that features associated with photon emission are easier to identify in the I-V's than features associated with absorption. Since the emission peaks are found at higher bias voltages than the corresponding absorption peaks, they occur in bias regions with little background due to lower-order processes. On the other hand, in the bias region where the n-photon absorption peak is expected, there is also a significant contribution due to the $(n-1)$-photon emission peak. Except for the case $n=1$, the position of the absorption peaks can thus not unambiguously be extracted from the I-V curves.

A comparison of the experiments and Tucker's theory for PAT at a frequency of 1.5 THz is shown in Figs. 4(a),(b). The theoretical curves have been calculated with the instantaneous I-V (dashed line) and Eq. (1) for $\alpha=0.9$, 1.1, 1.3, 1.6, and 2. It is apparent that Tucker's theory describes all essential features of the experimental data very well, including absolute negative conductance near the origin, and the opening of one-photon and two-photon emission channels at the appropriate bias voltages. The experimental picture looks entirely different at a frequency of 600 GHz [Fig. 4(c)]. There, only a single peak is observed that shifts continuously to higher bias voltages with increasing ac field. This is in sharp contrast to the behavior of the photon-assisted peaks in Fig. 4(a), whose position is independent of the ac field strength. Around zero bias several small steps are found at voltages where PAT peaks would be expected. Figure 4(d) shows the prediction of Tucker's theory for a photon energy $\hbar\omega=$ meV. It shows the same features as the experimental data, a continuously shifting main peak, and some fine structure at lower bias.

A calculation of the classical limit with Eq. (2) shows that both the 600-GHz data and the calculation with Tucker's theory look like classical rectification plus some remnants of quantum response around zero bias [Fig. 4(e)]. The shifting main peak in the classical limit may at first be surprising, but is a natural expression of the fact that in our experiments the ac fields are not small compared to the dc field. For a voltage bias $V_0+V_1\cos\omega t$ the current near the turning points $V_0\pm V_1$ gives the largest contribution to the time averaged dc current. Therefore, a peak in the modulated I-V is encountered whenever the excursion of the ac field just hits a peak in the unmodulated I-V.

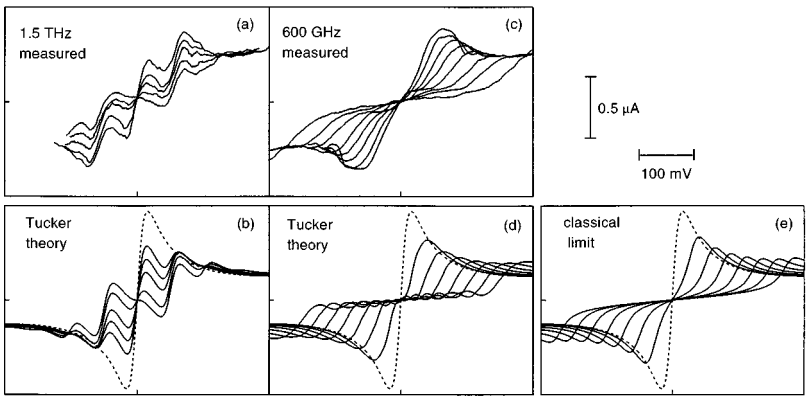

FIG. 4. Irradiated *I-V*'s for different power levels at (a) 1.5 THz and (c) 600 GHz, and the prediction of Tucker's theory using the proposed instantaneous *I-V* (dashed line) as input [(b), (d)]. The response in the classical limit is shown in (e). The origin is located in the center of each panel.

The data shown in Fig. 4 can therefore be interpreted as a transition from PAT (quantum response) at frequencies $\gtrsim$ THz to classical rectification at lower frequencies. At 600 GHz the response shows the essential features of classical rectification but some remnants of the quantum response are still present. At a lower frequency, ν=420 GHz, even these steps have completely disappeared. The transition in this frequency range can also be understood from a microscopic point of view. The scale of the nonlinearity in the instantaneous *I-V* is set by the ground-state level width $\Gamma \approx 2$ meV in a single quantum well. According to Tucker,[1] the transition from classical to quantum behavior is then expected for a photon energy $\hbar\omega \sim \Gamma$ or at about 500 GHz, in good agreement with the experimental results.

In conclusion, we have observed a transition from classical to quantum (PAT) response in a sequential resonant tunneling superlattice. We have suggested a consistent interpretation of the data using the instantaneous current-voltage characteristics of the superlattice to describe the high-frequency response. Below ~600 GHz the response can be well described by classical rectification, at higher frequencies multiphoton-assisted transport channels open, while direct tunneling may be significantly suppressed. This leads to the observation of absolute negative conductance near zero bias and, perhaps more important, to gain for frequencies just below the Stark splitting of the quantum well ground states. An improved understanding of the absorption and gain processes may contribute to future THz solid-state detectors and sources.

The authors would like to thank the staff at the Center for Free-Electron Laser Studies, J.R. Allen, D. Enyeart, G. Ramian, and D. White. Funding for the Center for Free-Electron Laser studies is provided by the Office of Naval Research. This research was also supported by the NSF, the Army Research Office, and the Air Force Office of Scientific Research. One of us (S.Z.) acknowledges financial support by the Deutsche Forschungsgemeinschaft (DFG).

[1] J.R. Tucker, IEEE J. Quantum Electron. **QE-15**, 1234 (1979); J.R. Tucker and M.J. Feldman, Rev. Mod. Phys. **57**, 1055 (1985).
[2] A.H. Dayem and R.J. Martin, Phys. Rev. Lett. **8**, 246 (1962).
[3] R.W. van der Heijden, S.M. Swartjes, and P. Wyder, Phys. Rev. B **30,** 3513 (1984).
[4] P.S.S. Guimaraes, B.J. Keay, J.P. Kaminski, S.J. Allen, Jr., P.F. Hopkins, A.C. Gossard, L.T. Florez, and J.P. Harbison, Phys. Rev. Lett. **70**, 3792 (1993).
[5] H. Drexler, J.S. Scott, S.J. Allen, K.L. Campman, and A.C. Gossard, Appl. Phys. Lett. **67**, 2816 (1995).
[6] L.P. Kouwenhoven, S. Jauhar, J. Orenstein, P.L. McEuen, Y. Nagamune, J. Motohisa, and H. Sakaki, Phys. Rev. Lett. **73**, 3443 (1994).
[7] B.J. Keay, S. Zeuner, S.J. Allen, Jr., K.D. Maranowski, A.C. Gossard, U. Bhattacharya, and M.J.W. Rodwell, Phys. Rev. Lett. **75**, 4102 (1995).
[8] P.K. Tien and J.P. Gordon, Phys. Rev. **129**, 647 (1963).
[9] C.A. Hamilton and S. Shapiro, Phys. Rev. B **2**, 4494 (1970).
[10] A.N. Korotkov, D.V. Averin, and K.K. Likharev, Phys. Rev. B **49**, 7548 (1994).
[11] K.K. Choi, B.F. Levine, R.J. Malik, J. Walker, and C.G. Bethea, Phys. Rev. B **35**, 4172 (1987).
[12] A. Wacker, F. Prengel, and E. Schöll, in *Physics of Semiconductors: Proceedings of the 22nd International Conference*, edited by D.J. Lockwood (World Scientific, Singapore, 1995), Vol. 2, p. 1075.
[13] B. Ricco and M.Ya. Azbel, Phys. Rev. B **29**, 1970 (1984); V.J. Goldman, D.C. Tsui, and J.E. Cunningham, *ibid.* **35**, 9387 (1987).
[14] E.E. Mendez, in *Physics and Applications of Quantum Wells and Superlattices*, edited by E.E. Mendez and K. von Klitzing (Plenum, New York, 1987), p. 159.